

E. J. Rohling · P. A. Mayewski · R. H. Abu-Zied  
J. S. L. Casford · A. Hayes

## Holocene atmosphere-ocean interactions: records from Greenland and the Aegean Sea

Received: 12 April 2001 / Accepted: 18 July 2001 / Published online: 8 February 2002  
© Springer-Verlag 2002

**Abstract** We compare paleoclimate proxy records from central Greenland and the Aegean Sea to offer new insights into the causes, timing, and mechanisms of Holocene atmosphere-ocean interactions. A direct atmospheric link is revealed between Aegean sea surface temperature (SST) and high-latitude climate. The major Holocene events in our proxies of Aegean SST and winter/spring intensity of the Siberian High (GISP2  $K^+$  record) follow an  $\sim 2300$  year spacing, recognised also in the  $\Delta^{14}C$  record and in worldwide Holocene glacier advance phases, suggesting a solar modulation of climate. We argue that the primary atmospheric response involved decadal-centennial fluctuations in the meridional pressure gradient, driving Aegean SST events via changes in the strength, duration, and/or frequency of northerly polar/continental air outbreaks over the basin. The observed natural variability should be accounted for in predictions of future climate change, and our time-frame for the Aegean climate events in addition provides an independent chronostratigraphic argument to Middle Eastern archaeological studies.

### 1 Introduction

Study of the Holocene (current interglacial, last  $\sim 11500$  years) allows assessment of climatic variability through the early to fully developed interglacial state during which modern climatic and geographic boundary con-

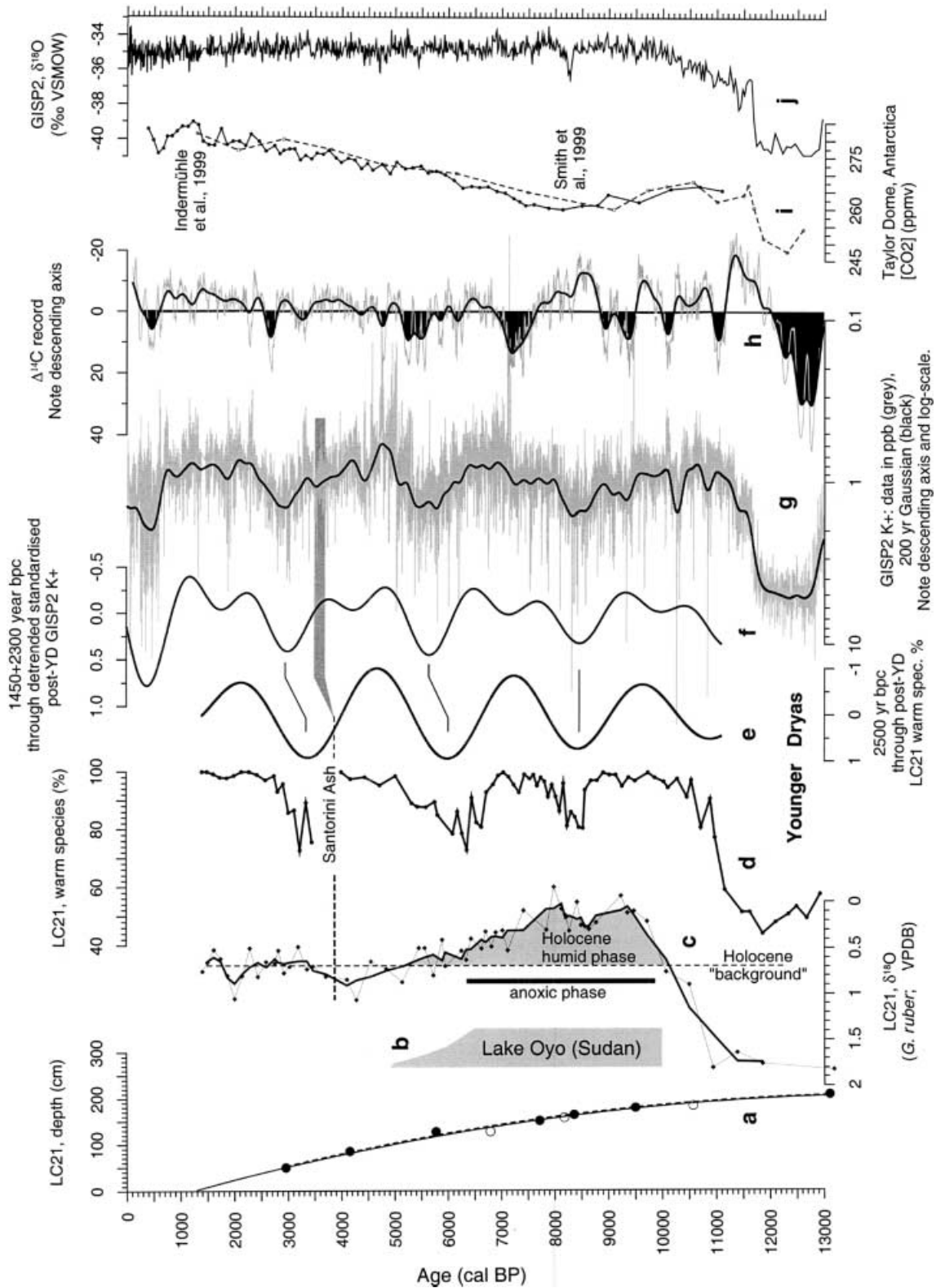
ditions have evolved. To assess direct atmosphere-ocean interactions during the Holocene, we compare the excellently dated record of atmospheric chemistry from the Greenland summit GISP2 ice core (72.6°N, 38.5°W; +3200 m) with an SST proxy record from an Aegean Sea (NE Mediterranean) sediment core (35.66°N, 26.58°E; -1522 m). This focus on the Aegean Sea is driven by the fact that it is a marginal sea with virtually no direct forcing by the North Atlantic thermohaline circulation (THC), and which is unaffected by sea-ice related complications (e.g. insolation, albedo effects). Due to its small volume, the Aegean lacks the inertia of larger ocean basins, allowing direct rather than lagged responses to forcing and well-developed signal amplitudes. Strong winter cooling due to orographically channelled northerly outbreaks of polar/continental air forms a dominant characteristic of the Aegean SST regime (Theocharis and Georgopoulos 1993; Poulos et al. 1997). This process is related to the vigour and southward extent of (sub)polar climate conditions over the Eurasian continent, and hence to the intensity of the Siberian High. Therefore, a direct relationship is expected between our Aegean SST proxy and the GISP2  $K^+$  series, which we argue to be a reliable proxy for winter/spring intensity of the Siberian High. The Aegean Sea therefore provides an ideal natural laboratory for assessment of direct hydrographic responses to high-latitude climate variability, for comparison with more complex fluctuations in THC- and ice-dominated regions.

### 2 Material and methods

The GISP2  $K^+$  proxy for intensity of the Siberian High (Fig. 1f) is based on the identification of strong relationships (summarised later, after Meeker and Mayewski in press) between high-resolution glaciochemical time series from central Greenland (Mayewski et al. 1997), and 1899–1987 AD instrumental records of atmospheric sea level pressure (SLP) over the North Atlantic and Asia (Trenberth and Paolino 1980). Given their seasonal deposition patterns in Greenland snow (e.g. winter/spring  $K^+$  maxima; Legrand and Mayewski 1997) annual ion concentration values are strongly

E. J. Rohling (✉) · R. H. Abu-Zied · J. S. L. Casford · A. Hayes  
School of Ocean and Earth Science,  
Southampton Oceanography Centre,  
Southampton SO14 3ZH, UK  
E-mail: E.Rohling@soc.soton.ac.uk

P. A. Mayewski  
Climate Studies Centre,  
Institute for Quaternary Studies and  
Department of Geological Sciences,  
University of Maine, Orono, Maine 04469, USA



influenced by variations in seasonal atmospheric circulation. Relative to years of low  $K^+$  deposition, years with high  $K^+$  deposition are associated with winter/spring strengthening of the high over Siberia, the coldest air mass in the Northern Hemisphere; the  $K^+$  and Siberian High series are positively correlated, sharing 58% of their variance (Meeker and Mayewski in press). Potassium is

transported in the finest range of Asian dust (Zhang et al. 1993), which enables long distance transport to Greenland (Biscaye et al. 1997).

The time-stratigraphic framework for the relevant interval of our SE Aegean core LC21 (Fig. 1a) represents a best fit through eight calibrated AMS $^{14}C$  datings (Mercone et al. 2000) (calibration



**Fig. 1.** **a** Time-stratigraphic framework for Aegean core LC21. Depth scale adjusted for the 10 cm thickness of the ash layer from the Minoan eruption of Santorini. *Solid line* is 2<sup>nd</sup> order polynomial fit through all *dots*, *dashed line* through *solid dots only*. *Solid dots* represent the seven youngest calibrated AMS<sup>14</sup>C datings of clean handpicked planktonic foraminifera from LC21 (Mercone et al. 2000). The framework presented here also uses a further dating for LC21, at 242.5 cm (Mercone et al. 2000), with a calibrated value of 16.66 ka BP. *Open dots* are similar datings for nearby core SL31, correlated into LC21 on the basis of high-resolution foraminiferal records for both cores. All datings were calibrated with Calib 4.1, the web-based updated version of the radiocarbon calibration program originally presented by Stuiver and Reimer (1993). An Aegean reservoir age correction of 150 years is applied (Facorellis et al. 1998). Note that the chronostratigraphic frameworks for the two options (one including, one excluding ages from SL31) are virtually identical. **b** Interval of presence of a lake in Oyo depression (NW Sudan), marking the early Holocene monsoonal maximum. Tapered end schematically represents the gradual aridification of Oyo Lake (Ritchie et al. 1985); **c** Oxygen isotope record for the summer mixed-layer dweller *Globigerinoides ruber* in LC21 (in ‰ VPDB). *Bold line* represents 3-point moving average that reduces noise. The Holocene background level is approximated at about the mean value of the last 2 kyr covered by the record. An excess depletion (*grey*) marks the enhanced freshwater flux into the Mediterranean during the monsoonal maximum (see Rohling 1999). *Black bar* indicates the extent of anoxic sedimentation in LC21 that corresponds to a widespread early Holocene phase of eastern Mediterranean deep water stagnation (e.g. Rohling et al. 1993, 1997; Myers et al. 1998; De Rijk et al. 1999; Hayes et al. 1999; Myers and Rohling 2000; Mercone et al. 2000, 2001). **d** Warm-cold plot for LC21, showing Holocene cool events representing relative winter SST reductions of the order of 2–4°C (see text). **e** 2500 ± 250 year bandpass filtering component through the linearly detrended Holocene portion of the record shown in **d**. Between **e** and **f**, *tie-lines* are indicated that relate peak ‘cold events’ in the bandpass components for the LC21 warm-cold plot and the GISP2 K<sup>+</sup> series. The inferred offsets are corroborated by the (*grey band*) *tie-line* for the Minoan eruption of Santorini (Bruins and Van der Plicht 1996; Kuniholm et al. 1996; NB. the strong 1623 ± 36 BC sulfate peak in GISP2 cannot further constrain this correlation, since associated ash-shards are non-Minoan (Zielinski and Germani 1998)). **f** Composite of 1450 and 2300 (± 10%) year bandpass components through the detrended Holocene portion of the GISP2 K<sup>+</sup> record (*solid line*) (for frequency analysis, see Mayewski et al. 1997). **g** GISP2 K<sup>+</sup> ion series (log-scale). The concentration axis is *printed in reverse* for consistency with the other records presented. *Grey* shows the data in ppb, *black* a 200 year moving Gaussian for main trends. **h** Global Δ<sup>14</sup>C record (*grey*; Stuiver et al. 1998), with definition of long-term trends by means of a 200-year moving Gaussian (*heavy black line*). Long-term positive excursions are *highlighted in black*. **i** Atmospheric CO<sub>2</sub> concentrations from analyses on Taylor Dome ice core, Antarctica (Indermühle et al. 1999; Smith et al. 1999)

details in the caption of Fig. 1a). It is corroborated by three further calibrated AMS<sup>14</sup>C datings, correlated into LC21 from nearby core SL31 on the basis of high-resolution foraminiferal records (available on request). Refinement is possible using the established age-range of 3.57 ± 0.08 ka BP for the Minoan eruption of Santorini (Bruins and Van der Plicht 1996; Kuniholm et al. 1996), and signal-correlation with the GISP2 K<sup>+</sup> series (see tie-lines between Fig. 1e and f and discussion).

The record of relative SST changes in LC21 (Fig. 1d) is based on planktonic foraminiferal abundance data with an average Holocene resolution of ~125 years. It represents a relative abundance (%) plot of “warm” versus “cool” species (cf. Rohling et al. 1997; De Rijk et al. 1999), based on modern habitat characteristics discussed in Hemleben et al. (1989), Rohling et al. (1993), Pujol and Vergnaud-Grazzini (1995), and Reiss et al. (2000). The “warm”

group consists of the photosynthetic symbiont-bearing spinose species *Globigerinoides ruber* (pink + white), *Orbulina universa*, *Globigerinoides sacculifer*, *Globigerinella siphonifera*, *Globoturbotalita rubescens*, and *Globoturbotalita tenella*, with traces of *Hastigerina pelagica* and *Globigerinella digitata*. Today, this association dominates warm and oligotrophic summer mixed layers in subtropical regions, including the easternmost Mediterranean. The “cool” group comprises the non-spinose species *Globoturbotalia scitula*, *Turbotalita quinqueloba*, *Globoturbotalia inflata*, and *Neogloboquadrina pachyderma* (right-coiling). These lack symbionts, show a herbivorous feeding preference, and thrive in the cool, more eutrophic conditions fuelled by upmixing of regenerated nutrients in winter mixed layers (*G. scitula*, *T. quinqueloba*, *G. inflata*), or in the previous winters’ water below the summer thermocline *N. pachyderma*. Due to small available sample volumes and very low post ~6 ka BP organic carbon contents, there is no supporting alkenone SST record for LC21. However, previous studies support the validity of relative SST trends from our basic faunal proxy, showing similar trends in records based on elaborate statistical transformations, dinoflagellate abundance data, and Uk’37 (Rohling et al. 1993; Targarona et al. 1997; Cacho et al. 1999, 2000, 2001; De Rijk et al. 1999; Hayes et al. 1999; Paterne et al. 1999).

Absolute calibration of faunal SST proxies remains controversial because of the potential impacts of additional physico-chemical influences on abundance patterns (e.g. food availability). In fact the ratio used here would be more aptly described as a reflection of the prevalence of summer stratification, but since this is intimately linked to temperature, the ratio can be used to obtain first-order estimates of SST change. The bulk of the warm, oligotrophic, eastern Mediterranean shows very high values above 90%, but certain limited regions show lower values, down to ~70%. Such values are attained in regions of pronounced winter cooling, with deeper and more intensive winter overturn than in most of the eastern Mediterranean, and the northern Aegean is such a region. Figure 2 illustrates that the gradient in warm species percentage values observed in core-top sediments (Thunell 1978, 1979) closely relates to the present-day winter SST gradient in the Aegean Sea (Poulos et al. 1997). Core LC21’s location at the present-day boundary between the cooler Aegean regime and the warmer Levantine conditions assures a sensitive response in the SST proxy.

We contend that the Holocene alternation between intervals with ~100% and intervals with ~80% scores on our faunal proxy (Fig. 1d) allows a sufficiently accurate first-order reconstruction of relative changes in winter temperature/hydrographic conditions. We simply consider that ~100% intervals were characterised by temperature/hydrographic conditions similar to those in nearby modern areas where such scores are attained (the Levantine Basin), and that intervals with scores ~80% were characterised by temperature/hydrographic conditions found in nearby modern areas with such values in the faunal proxy (the northernmost Aegean) (Fig. 2).

Frequency analysis for the Holocene part of the GISP2 K<sup>+</sup> series was discussed extensively in Mayewski et al. (1997), and the bandpass components (bpc) of 1450 and 2300 years detected in that study are presented in Fig. 1f. We here present a similar analysis for the Holocene Aegean SST proxy. First we linearly interpolated the record, to read values at evenly spaced intervals of one decade. Next, we linearly detrended the decadal interpolated data. This was followed by calculation of a maximum entropy spectrum from the autocorrelation matrix as determined over N/4 lags. The results were considered in a logarithmic plot of variance density, and confidence limits determined using the χ<sup>2</sup> distribution. A broad peak was observed at 0.4 cycles kyr<sup>-1</sup>. Being based on only three effective cycles, the spectral analysis is not entirely conclusive for this frequency. In validation, the spacing of the significant correlation maxima in a complete autocorrelation series was considered (mean spacing: 262 decadal lags between three highly significant correlation maxima). The bandpass component (bpc) presented in Fig. 1e is based on a Blackman-type bandpass filter using a window of 0.4 ± 0.04 cycles kyr<sup>-1</sup>.

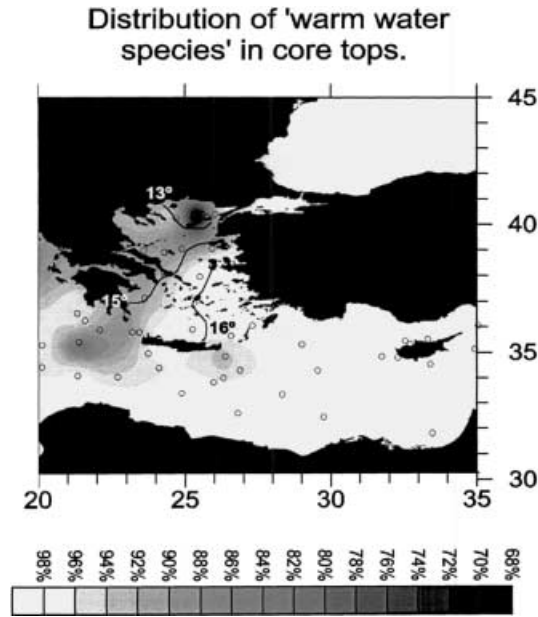


**Fig. 2.** Map of the Aegean Sea and adjacent Levantine Sea, with warm species percentage scores following the method discussed in the text, based on the core-top faunal descriptions of Thunell (1978, 1979). Solid black lines indicate the positions of the present-day 13, 15, and 16 °C surface water isotherms in winter (Poulos et al. 1997)

### 3 Nature of Aegean cooling events

The ~100% warm fauna in core LC21 resembles that found today in the southeast Mediterranean Levantine basin, where minimum SST remains above 16 °C (Hecht, 1992; Pujol and Vergnaud-Grazzini, 1995; Reiss et al. 2000). In contrast, the faunas in the cool intervals are rather similar to those in the present-day northernmost Aegean (Fig. 2), and tend towards those commonly observed in winter in the western Mediterranean Provençal and Catalan basins where temperatures range between 12.5 and 14 °C (Pujol and Vergnaud-Grazzini, 1995; Rohling et al. 1995). Winter conditions in the Aegean Sea are strongly affected by northerly outbreaks of cold and dry polar/continental air over the basin, funnelled through the valleys of the rivers Axios (Vardar zone), Strimon, and Evros, causing minimum temperatures of 12–14 °C in the north to ~16 °C in the southerly site of core LC21 (Theocharis and Georgopoulos, 1993; Poulos et al. 1997).

We interpret the Holocene cool events in LC21 (Fig. 1d) in terms of long-term (multi-decadal) periods of increased intensity, duration, and/or frequency of the winter-time northerly air outbreaks, causing winter conditions that today are restricted to the northern sector of the basin to intensify and expand southward over the Aegean Sea. As a consequence, the northerly “Aegean type” regime significantly affected the SE Aegean site of LC21 during the cool events, while episodes with ~100% warm fauna in LC21 reflect a strong dominance of southerly “Levantine type” conditions. This reconstruction implies that the Holocene cool

events were characterised by 2–4 °C winter SST reductions throughout the Aegean. The inferred magnitude of the Holocene cooling events compares favourably with that found with the Uk’37 method for the western Mediterranean (Cacho et al. 1999; 2000; 2001). Note that those studies also related the western Mediterranean cooling events to intensified orographically channelled northerly air outbreaks, supporting the initial identification of this mechanism’s importance for intense NW Mediterranean cooling during Atlantic Heinrich events (Rohling et al. 1998).

Our inference that the Aegean cooling events were predominantly winter phenomena is corroborated by the very muted responses in the stable oxygen isotope record of the summer mixed-layer dweller *G. ruber* (Fig. 1c). Short-lived winter cooling events would leave negligible residual signals in the strongly heated summer mixed layer, and, in general, the isotope record through the early-mid Holocene is strongly dominated by changes in the basin’s hydrological constraints (see Rohling 1999). We emphasise that both observations in the modern Aegean Sea (Roether et al. 1996; Klein et al. 1999), and numerical simulations of eastern Mediterranean palaeo-circulation (Myers and Rohling 2000), show that even minor winter SST decreases would have profound impacts on the local hydrography, driving increased rates of local deep-water formation that impact on ventilation of the entire eastern Mediterranean.

### 4 Temporal Relationship Between LC21 and GISP2

Before possible climatic relationships can be discussed, the event timing and structure of the Aegean SST proxy record needs to be compared carefully with that of the GISP2  $K^+$  proxy for winter/spring intensity of the Siberian High (Fig. 1d–g). The structure of the bandpass components (Fig. 1e,f) suggests in-phase behaviour of the main Holocene variability (2.3–2.5 kyr cycle) in the early Holocene portion of the two records, but shows a 300 to 400 year offset in the middle to late Holocene that would suggest a minor phase lag (tie-lines between Fig. 1e and f). However, we argue that these offsets are *not* real phase differences, but instead result from minor inconsistencies in the chronostratigraphic framework of LC21. This is clearly witnessed by the fact that the age of the Minoan ash layer in LC21 (~3.9 ka BP) appears too old by the same 300–400 year difference, relative to its actual age of  $3.57 \pm 0.08$  ka BP (Bruins and Van der Plicht 1996; Kuniholm et al. 1996) (dashed line to grey band through Fig. 1c–g). Since the core has been adequately dated in the interval in question, and since the dating technique’s analytical precision is an order of magnitude more accurate than the apparent offsets, other processes must be considered that could have introduced a bias of up to several centuries in the datings.

The limiting factor on the quality of AMS  $^{14}C$  datings of foraminiferal shells from sediment samples is not analytical precision, but the nature of the material dated.

Several processes may introduce bias, such as syn-sedimentary admixture of older shells (e.g. eroded from the basin's extensive shelf/slope areas), poorly constrained reservoir-age corrections, or bioturbational admixture of previously deposited material with more recently deposited material. We infer that bioturbation effects were particularly important in causing the 300 to 400 year offset in the younger part of LC21 (around the Minoan ash; see earlier), since there is no such offset for the event centred at  $\sim 8.4$  ka BP, which resides within an interval of severe bottom-water dysoxia (sapropel S1) that impeded benthic life and so suppressed bioturbation (Mercone et al. 2001). The actual data (Fig. 1d,g), rather than the bandpass components, suggest a greatest apparent offset between LC21 and GISP2 of  $\sim 500$  years for the event centred on 5.5 ka BP in GISP2. The equivalent event in LC21 marks the eastern Mediterranean reventilation after the S1 stagnant/anoxic deep-water episode (see Rohling et al. 1997; Myers et al. 1998; De Rijk et al. 1999; Hayes et al. 1999; Mercone et al. 2000; 2001) that corresponded to the early Holocene monsoon maximum (Fig. 1b,c). Dated carbonates from this interval are likely to reflect some admixture of old carbon from previously stagnant parts of the water column (i.e. the reservoir age was higher than we have assumed).

These arguments, with particular emphasis on the discrepancy in the age of the Minoan ash, leads us to conclude (1) that the apparent age offsets between the Aegean and GISP2 records are *not* genuine phase lags but the result of minor complications in the radiocarbon framework of LC21, and (2) that the main variability in the Aegean record highlighted by the bpc consequently shows a high degree of correspondence in both event timing and structure with that of the GISP2  $K^+$  proxy for winter/spring intensity of the Siberian High (Fig. 1e,f).

## 5 Discussion and conclusions

The  $\sim 1450$  year quasi-cyclicity that strongly dominates the glacial part of the GISP2  $K^+$  record is only weakly represented in the Holocene (Mayewski et al. 1997). The Holocene section shows a much more powerful  $\sim 2300$  year cycle (Fig. 1f,g), which is also present in the  $\Delta^{14}C$  residual series (Stuiver and Braziunas 1993; Mayewski et al. 1997). We find a basic periodicity in the Holocene Aegean SST proxy record around 2500 year (Fig. 1e). The Aegean record offers no evidence for a pervasive  $\sim 1450$  year periodicity such as that described from Glacial and Holocene ice rafted debris records in the North Atlantic (Bond et al. 1997; 1999), and from Holocene drift deposits in the North Atlantic Deep Water overflow region (Bianchi and McCave 1999). We consider the widespread dominance of the  $\sim 1450$  year cyclicity in palaeoclimate proxy records of the last glacial cycle (overviews in Boyle 1997; Broecker 2000; and references therein) to be suggestive of amplified environmental responses, involving the thermohaline circulation (THC), in a world bound by glacial boundary conditions.

Coral records show that the Northern Hemisphere was only deglaciated to its present extent by  $\sim 7$  ka BP (Blanchon and Shaw 1995), and the associated deceleration of sea level change is corroborated by widespread delta initiation around that time (Stanley and Hait 2000). The disappearance of the glacial ice would have minimised ice-related feedback processes responsible for amplified expression of the  $\sim 1450$  year cycle, so that only North Atlantic sites directly affected by the THC and any remaining continental ice (Greenland) continued to record its weak influence through the Holocene (Bond et al. 1997; 1999; Bianchi and McCave 1999). Virtually isolated from the influences of the THC and remaining ice, the Aegean experienced no residual  $\sim 1450$  year variability during the Holocene, but instead recorded some fundamental  $\sim 2300$  to 2500 year cycle (Fig. 1d,e).

What is the nature of this roughly 2300 year cycle observed in both the GISP2  $K^+$  and Aegean SST series? It is very similar to the  $\sim 2500$  year global cooling cycle illustrated by Holocene glacier advances in Europe, N America, New Zealand (Denton and Karlen 1973) and central Asia (summary in Zhang et al. 2000). It obviously is not related to any systematic variability in the atmospheric  $CO_2$  record (Indermühle et al. 1999; Smith et al. 1999; Fig. 1i). Within the interval since 7 ka BP (i.e. since completion of the deglaciation), however, there is a good match of each of the  $\sim 2300$  year spaced events in our records with longer-term peaks in the  $\Delta^{14}C$  residual series, which are associated with triplet  $\Delta^{14}C$  episodes (Stuiver and Braziunas 1989, 1993; O'Brien et al. 1995; Stuiver et al. 1998; Fig. 1h). This correspondence cannot be explained in terms of THC variability since THC-intensity proxies are considered to show variability not of  $\sim 2300$  years but of  $\sim 1500$  years (Bianchi and McCave 1999). During the early Holocene prior to 7 ka BP, our records suggest a completely different phase-relationship with the  $\Delta^{14}C$  series than after 7 ka BP. We tentatively suggest that this might be a function of stronger Northern Hemisphere ice dynamics and associated THC variability prior to 7 ka BP. We refrain from further speculations in view of the limited amount of global information that is available about the Holocene intensity and/or structure of ocean circulation.

Even within the post-7 ka BP interval, the match of the  $\Delta^{14}C$  anomalies and the atmospheric circulation changes reflected in the GISP2  $K^+$  series is not unequivocal when considered in detail (Fig. 1h,g). There either are small offsets in the age-models for these two proxies, or changes in the mixing between the various carbon reservoirs within the circulation/climate system contributed significantly to the  $\Delta^{14}C$  signals (see also Magny 1993). The latter contribution cannot be resolved until a truly global synthesis of Holocene ocean/climate variability is generated, but Bianchi and McCave's (1999) recent insight into North Atlantic THC variability suggests that at least the involvement of that major system can be discounted. Combining our findings with a previous assessment (Van Geel 1999), and considering the striking agreement that exists between

the  $^{10}\text{Be}$  (Finkel and Nishiizumi 1997) and  $\Delta^{14}\text{C}$  records, we suggest that the global  $\sim 2300$  year cycle in the Holocene reflects a primary forcing mechanism, which could be anchored in solar variability. Our results suggest that this forcing affected the physical environment via reorganisation in the atmospheric circulation, conducive to long-term (multi-decadal) enhancement of winter conditions over the Eurasian continent, with consistently enhanced pressure in the winter/spring Siberian High over decades to centuries and enhanced polar/continental air outbreaks over the Aegean Sea.

In view of these findings, we call for an in-depth multi-disciplinary assessment of the potential for solar modulation of climate on centennial scales. Potential mechanisms for transmission of solar variability to climate change were discussed by Van Geel et al. (1999) and Beer et al. (2000). Moreover, a climate model suggested that in/decreases in stratospheric ozone production, due to in/decreases in UV radiation, would lead to warming/cooling of the lower stratosphere, which in turn would affect the meridional extent of atmospheric cells (Haigh 1996). Since this is exactly the type of reorganisation in the climate system that was inferred previously to explain the GISP2 ion series (i.e. the Polar Circulation Index for strength and extent of the polar vortex; Mayewski et al. 1997) and which is further supported in the present study, we consider that targeted investigations of Haigh's (1996) mechanism are particularly relevant. As stated also by Magny (1993), extrapolation of the observed natural variability into the future suggests a high probability for a distinct natural warming trend over the next few centuries that would intensify any anthropogenic greenhouse effects.

Finally, we note that our reconstruction (a) signals the importance of the incorporation of appropriate modes and time scales of natural climate variability in models for future climate predictions, and (b) offers narrow constraints to the timing and sequence of major Holocene climate events near the Middle East that may help in constraining the chronologies of archaeological records from this region.

**Acknowledgements** We thank: the two anonymous reviewers for valuable suggestions; I. Cacho, J. Thomson and F.J. Jorissen for stimulating discussions; M. Sarnthein and J. Kennett for organising the February 2000 SCOR-IMAGES workshop in Trins (Austria) where we first compared the records presented here; and Steve Cooke and Connie de Vries for their efforts concerning the stable isotope analyses of LC21 at the SOC stable isotope facility. Datings for LC21 (after Mercone et al. 2000) and for SL31 (after Casford et al. in press), as well as foraminiferal relative abundance data for both cores, may be requested from E.Rohling@soc.soton.ac.uk. Data for Fig. 1g-j are held at the National Snow and Ice Data Center, University of Colorado at Boulder, and the WDC-A for Paleoclimatology, National Geophysical Data Center, Boulder, Colorado, USA.

## References

Beer J, Mende W, Stellmacher R (2000) The role of the sun in climate forcing. *Quat Sci Rev* 19: 403–415

- Bianchi GG, McCave IN (1999) Holocene periodicity in North Atlantic climate and deep-ocean flow south of Iceland. *Nature* 397: 515–517
- Biscaye PE, Grousset FE, Revel M, Van der Gaast S, Zielinski GA, Vaars A, Kukla G (1997) Asian provenance of glacial dust (stage 2) in the Greenland Ice Sheet Project 2 ice core, Summit, Greenland. *J Geophys Res* 102: 26765–26782
- Blanchon P, Shaw J (1995) Reef drowning during the last deglaciation: evidence for catastrophic sea-level rise and ice-sheet collapse. *Geology* 23: 4–8
- Bond G, Showers W, Cheseby M, Lotti R, Almasi P, deMenocal P, Priore P, Cullen H, Hajdas I, Bonani G (1997) A pervasive millennial-scale cycle in North Atlantic Holocene and Glacial climates. *Science* 278: 1257–1266
- Bond GC, Showers W, Elliot M, Evans M, Lotti R, Hajdas I, Bonani G, Johnson S (1999) The North Atlantic's 1–2 kyr climate rhythm: relation to Heinrich events, dansgaard/Oeschger cycles and the little ice age. In: Clark PU, Webb RS, Keigwin LD (eds) Mechanisms of global climate change at millennial time scales. AGU Geophysical Monograph 112, pp 35–58, American Geophysical Union, Washington DC
- Boyle EA (1997) Characteristics of the deep ocean carbon system during the past 150000 years:  $\Sigma\text{CO}_2$  distributions, deep water flow patterns, and abrupt climate change. *Proc Natl Acad Sci USA* 94: 8300–8307
- Broecker WS (2000) Abrupt climate change: causal constraints provided by the paleoclimate record. *Earth-Sci Rev* 51: 137–154
- Bruins HJ, Van Der Plicht J (1996) The exodus enigma. *Nature* 382: 213–214
- Cacho I, Grimalt JO, Canals M, Sbaifi L, Shackleton NJ, Schönfeld J, Zahn R (2001) Variability of the western Mediterranean Sea surface temperatures during the last 25000 years and its connection with the northern hemisphere climatic changes. *Paleoceanography* 16: 40–52
- Cacho I, Grimalt JO, Pelejero C, Canals M, Sierro FJ, Flores JA, Shackleton N (1999) Dansgaard-Oeschger and Heinrich event imprints in Alboran Sea paleotemperatures. *Paleoceanography* 14: 698–705
- Cacho I, Grimalt JO, Sierro FJ, Shackleton NJ, Canals M (2000) Evidence of enhanced Mediterranean thermohaline circulation during rapid climate coolings. *Earth Planet Sci Lett* 183: 417–429
- Casford JSL, Rohling EJ, Abu-Zied R, Cooke S, Fontanier C, Leng M, Lykousis V (2001) Circulation changes and nutrient concentrations in the Late Quaternary Aegean Sea: a non-steady state concept for sapropel formation. *Paleoceanography*. (in press)
- Denton GH, Karlen W (1973) Holocene climatic variations – their pattern and possible cause. *Quat Res* 3: 155–205
- De Rijk S, Rohling EJ, Hayes A (1999) Onset of climatic deterioration in the eastern Mediterranean around 7 ky BP; micro-paleontological data from Mediterranean sapropel interruptions. *Mar Geol* 153: 337–343
- Facorellis Y, Maniatis Y, Kromer B (1998) Apparent  $^{14}\text{C}$  ages of marine mollusc shells from a Greek island: calculation of the marine reservoir effect in the Aegean Sea. *Radiocarbon* 40: 963–973
- Finkel RC, Nishiizumi K (1997) Beryllium 10 concentrations in the Greenland Ice Sheet Project 2 ice core from 3–40 ka. *J Geophys Res* 102: 26699–26706
- Haigh JD (1996) The impact of solar variability on climate. *Science* 272: 981–984
- Hayes A, Rohling EJ, De Rijk S, Zachariasse WJ (1999) Mediterranean planktonic foraminiferal faunas during the last glacial cycle. *Mar Geol* 153: 239–252
- Hecht A (1992) Abrupt changes in the characteristics of Atlantic and Levantine intermediate waters in the southeastern Levantine basin. *Oceanol Acta* 15: 25–42
- Hemleben C, Spindler M, Anderson OR (1989) Modern planktonic foraminifera. Springer, New York Berlin Heidelberg, pp 363
- Indermühle A, Stocker TF, Joos F, Fischer H, Smith HJ, Wahlen M, Deck B, Mastroianni D, Tschumi J, Blunier T, Meyer R, Stauffer B (1999) Holocene carbon-cycle dynamics based on

- CO<sub>2</sub> trapped in ice at Taylor Dome, Antarctica. *Nature* 398: 121–126
- Klein B, Roether W, Manca BB, Bregant D, Beitzel V, Kovacevic V, Luchetta A (1999) The large deep water transient in the eastern Mediterranean. *Deep-Sea Res* 46: 371–414
- Kuniholm PI, Kromer B, Manning SW, Newton M, Latini CE, Bruce MJ (1996) Anatolian tree rings and the absolute chronology of the eastern Mediterranean, 2220–718 BP. *Nature* 381: 780–783
- Legrand M, Mayewski PA (1997) Glaciochemistry of polar ice cores: a review. *Rev Geophys* 35: 219–143
- Magny M (1993) Solar influences on Holocene climatic changes illustrated by correlations between past lake-level fluctuations and the atmospheric <sup>14</sup>C record. *Quat Res* 40: 1–9
- Mayewski PA, Meeker LD, Twickler MS, Whitlow S, Yang Q, Prentice M (1997) Major features and forcing of high latitude northern hemisphere atmospheric circulation using a 110000-year-long glaciouchemical series. *J Geophys Res* 102: 26345–26366
- Meeker LD, Mayewski PA (2001) A 1400 year long record of atmospheric circulation over the North Atlantic and Asia. Holocene (in press)
- Mercione D, Thomson J, Abu-Zied RH, Croudace IW, Rohling EJ (2001) High-resolution geochemical and micropalaeontological profiling of the most recent eastern Mediterranean sapropel. *Mar Geol* 177: 25–44
- Mercione D, Thomson J, Croudace IW, Siani G, Paterne M, Troelstra S (2000) Duration of S1, the most recent sapropel in the eastern Mediterranean Sea, as indicated by accelerated mass spectrometry radiocarbon and geochemical evidence. *Paleoceanography* 15: 336–347
- Myers PG, Rohling EJ (2000) Modelling a 200 year interruption of the Holocene sapropel S1. *Quat Res* 53: 98–104
- Myers P, Haines K, Rohling EJ (1998) Modelling the paleo-circulation of the Mediterranean: the last glacial maximum and the Holocene with emphasis on the formation of sapropel S1. *Paleoceanography* 13: 586–606
- O'Brien SR, Mayewski PA, Meeker LD, Meese DA, Twickler MS, Whitlow SI (1995) Complexity of Holocene climate as reconstructed from a Greenland ice core. *Science* 270: 1962–1964
- Paterne M, Kallel N, Labeyrie L, Vautravers M, Duplessy J-C, Rossignol-Strick M, Cortijo E, Arnold M, Fontugne M (1999) Hydrological relationship between the North Atlantic ocean and the Mediterranean during the past 15–75 kyr. *Paleoceanography* 14: 626–638
- Poulos SE, Drakopoulos PG, Collins MB (1997) Seasonal variability in sea surface oceanographic conditions in the Aegean Sea (eastern Mediterranean): an overview. *J Mar Sys* 13: 225–244
- Pujol C, Vergnaud-Grazzini C (1995) Distribution patterns of live planktic foraminifers as related to regional hydrography and productive systems of the Mediterranean Sea. *Mar Micropaleontol* 25: 187–217
- Reiss Z, Halicz E, Luz B (2000) Late-Holocene foraminifera from the SE Levantine Basin. *Isr J Earth Sci* 48: 1–27
- Ritchie JC, Eyles CH, Haynes CV (1985) Sediment and pollen evidence for an early to mid-Holocene humid period in the eastern Sahara. *Nature* 314: 352–355
- Roether WH, Manca BB, Klein B, Bregant D, Georgopoulos D, Beitzel V, Kovacevic V, Luchetta A (1996) Recent changes in eastern Mediterranean deep waters. *Science* 271: 333–335
- Rohling EJ (1999) Environmental controls on salinity and delta-18O in the Mediterranean. *Paleoceanography* 14: 706–715
- Rohling EJ, Den Dulk M, Pujol C, Vergnaud-Grazzini C (1995) Abrupt hydrographic change in the Alboran Sea (western Mediterranean) around 8000 yrs BP. *Deep-Sea Res* 42: 1609–1619
- Rohling EJ, Jorissen FJ, De Stigter HC (1997) 200 year interruption of Holocene sapropel formation in the Adriatic Sea. *J Micropal* 16: 97–108
- Rohling EJ, Jorissen FJ, Vergnaud-Grazzini C, Zachariasse WJ (1993) Northern Levantine and Adriatic Quaternary planktic foraminifera; reconstruction of paleoenvironmental gradients. *Mar Micropaleontol* 21: 191–218
- Rohling EJ, Hayes A, Kroon D, De Rijk S, Zachariasse WJ, Eisma D (1998) Abrupt cold spells in the NW Mediterranean. *Paleoceanography* 13: 316–322
- Smith HJ, Fischer H, Mastroianni D, Deck B, Wahlen M (1999) Dual modes of the carbon cycle since the Last Glacial Maximum. *Nature* 400: 248–250
- Stanley DJ, Hait AK (2000) Deltas, radiocarbon dating, and measurements of sediment storage and subsidence. *Geology* 28: 295–298
- Stuiver M, Braziunas TF (1989) Atmospheric <sup>14</sup>C and century-scale solar oscillations. *Nature* 338: 405–408
- Stuiver M, Braziunas TF (1993) Sun, ocean, climate and atmospheric <sup>14</sup>CO<sub>2</sub>: an evaluation of causal and spectral relationships. *Holocene* 3: 289–305
- Stuiver M, Reimer PJ (1993) Extended <sup>14</sup>C data base and revised Calib 3.0 <sup>14</sup>C age calibration program. *Radiocarbon* 35: 215–230
- Stuiver M, Grootes PM, Braziunas TF (1995) The GISP2 180 climate record of the past 16500 years and the role of the sun, ocean and volcanoes. *Quat Res* 44: 341–354
- Stuiver M, Reimer PJ, Bard E, Beck JW, Burr GS, Hughen KA, Kromer B, McCormac FG, Van der Plicht J, Spurk M (1998) INTCAL98 Radiocarbon Age Calibration, 24000–0 cal BP. *Radiocarbon* 40: 1041–1083
- Targarona J, Boessekool K, Brinkhuis H, Visscher H, Zonneveld K (1997) Land-sea correlation of events in relation to the onset and ending of sapropel S1: a palynological approach. In: Targarona J (ed) Climatic and oceanographic evolution of the Mediterranean region over the last glacial-interglacial transition: a palynological approach, LPP Contributions Series. 7, Febo, Utrecht, NL pp 87–112
- Theocharis A, Georgopoulos D (1993) Dense water formation over the Samothraki and Limnos Plateaux in the north Aegean Sea (eastern Mediterranean Sea). *Cont Shelf Res* 13: 919–939
- Thunell RC (1978) Distribution of recent planktonic foraminifera in surface sediments of the Mediterranean Sea. *Mar Micropaleontol* 3: 147–173
- Thunell RC (1979) Eastern Mediterranean Sea during the last glacial maximum; an 18000 year BP reconstruction. *Quat Res* 11: 353–372
- Trenberth KE, Paolino DA. Jr (1980) The northern hemisphere sea level pressure data set: trends, errors and discontinuities. *Mon Weather Rev* 106: 855–872
- Van Geel B, Raspopov OM, Renssen H, Van Der Plicht J, Dergachev VA, Meijer HAJ (1999) The role of solar forcing upon climate change. *Quat Sci Rev* 18: 331–338
- Zhang XY, Arimoto R, An ZS, Chen T, Zhang GY, Shu G, Wang XF (1993) Atmospheric trace elements over source regions of Chinese dust: concentrations, sources and atmospheric input to the Loess plateau. *Atmos Environ* 27A: 2051–2067
- Zhang HC, Ma YZ, Wünnemann B, Pachur HJ (2000) A Holocene climatic record from arid northwestern China. *Palaeogeogr Palaeoclimatol Palaeoecol* 162: 389–401
- Zielinski G, Germani MS (1998) New ice-core evidence challenges the 1620s BC age for the Santorini (Minoan) eruption. *J Archaeol Sci* 25: 279–289